DOI: 10.1002/ejic.200700930

The Use of 2,1,3-Benzoselenadiazole as an Auxiliary Ligand for the Construction of New 2D Silver(I)/Benzene- or Cyclohexane-1,3,5-tricarboxylate Honeycomb Networks

Cheng-Kang Tan,[a] Jing Wang,[a] Ji-Dong Leng,[a] Ling-Ling Zheng,[a] and Ming-Liang Tong*[a]

Keywords: Silver / Selenium / Carboxylate ligands / Materials science / Organic-inorganic hybrid composites

The reaction of freshly synthesized $[Ag(NH_3)_2](OH)$, 2,1,3-benzoselenadiazole (bsd) and benzene- or cyclohexane-1,3,5-tricarboxylic acid (H_3btc/H_3ctc) results in two new coordination polymers containing 2D Ag_3(btc) and Ag_3(ctc) hexagonal motifs, namely $[Ag_3(btc)(bsd)_6]\cdot 0.5H_2O$ (**1**) and $[Ag_3(ctc)(bsd)_3]\cdot 1.5bsd\cdot 3.5H_2O$ (**2**). Complex **1** is a 3D supramolecular framework extended by deformed 2D Ag_3(btc) honeycomb nets via Se···N synthons formed between the dangling monodentate bsd groups, whereas **2** is a 3D metal–organic framework of nanoscale cages made up from ideal Ag_3(ctc) honeycomb layers and μ_2-bridging bsd ligands.

Introduction

Crystal engineering has provided a useful paradigm for the design of organic solids, supramolecular metal complexes and metal–organic frameworks (MOFs) with tunable properties containing different building blocks. Much of the recent progress in this area is based on the idea of self-assembly of tailor-made building blocks that are either organic molecules or metal complexes with polyfunctional organic ligands.[1–3] 1,3,5-Benzenetricarboxylic acid (H_3btc) and 1,3,5-cyclohexanetricarboxylic acid (H_3ctc), which have threefold symmetry, are inherently disposed to form hydrogen-bonded honeycomb sheets because their carboxyl groups tend to form cyclic hydrogen-bonded pairs in an $R^2_2(8)$ pattern (Scheme 1a). H_3btc and H_3ctc have been widely applied as archetypical organic scaffolds for the self-assembly of unary (containing only H_3btc) and binary (containing H_3btc linked in an ordered fashion to other molecules) hexagonal networks via hydrogen-bonding synthons with $R^2_2(8)$, $R^3_3(10)$ or $R^4_4(12)$ patterns.[4,5] The construction of a coordination polymer with a 2D M(btc/ctc) honeycomb motif is extremely challenging, although one can anticipate that the H atoms in the $R^2_2(8)$ pattern could be rationally replaced by metal ions. The silver(I) ion principally exhibits linear, trigonal, and tetrahedral coordination and has a high affinity for hard donor atoms such as nitrogen or oxygen atoms[6] and soft donor atoms such as sulfur atoms,[7] which makes it a favored and fashionable building block for MOFs. Furthermore, the silver ion is apt to form short Ag···Ag contacts as well as ligand-unsupported interactions, which have been proved to be two of the most important factors contributing to the formation of such complexes and their special properties.[8,9]

Unfortunately, it is difficult to control the symmetry of the resulting frameworks due to the silver(I) ion's rich coordination modes. A useful strategy in building such networks is therefore to employ an appropriate auxiliary ligand that can occupy one or more of the coordination sites of the metal ions and thereby prevent the formation of complicated frameworks. We decided to use 2,1,3-benzoselenadiazole (bsd), which may be a good candidate for the use as an auxiliary ligand but has only been used in a similar way in a previous report from our group.[10] Herein we report two novel silver coordination polymers that contain 2D Ag_3(btc) and Ag_3(ctc) hexagonal motifs, namely $[Ag_3(btc)(bsd)_6]\cdot 0.5H_2O$ (**1**) and $[Ag_3(ctc)(bsd)_3]\cdot 1.5bsd\cdot 3.5H_2O$ (**2**), respectively, and demonstrate a new and effective way to self-assemble hexagonal Ag^I(btc/ctc) coordination networks in the presence of 2,1,3-benzoselenadiazole (bsd) as the auxiliary ligand (Scheme 1b).

[a] State Key Laboratory of Optoelectronic Materials and Technologies, Institute of Optoelectronic and Composite Materials & School of Chemistry and Chemical Engineering, Sun Yat-Sen University,
Guangzhou 510275, China
Fax: +86-20-8411-2245
E-mail: tongml@mail.sysu.edu.cn

Supporting information for this article is available on the WWW under http://www.eurjic.org or from the author.

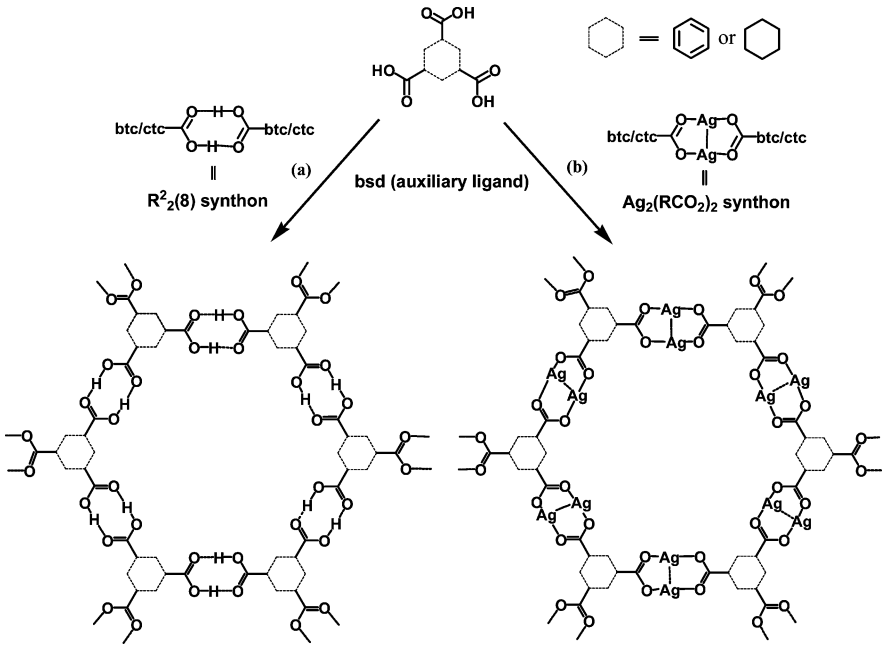

Scheme 1. Well-known 2D hexagonal net directed by the $R^2_2(8)$ hydrogen-bonded pattern (a) and our strategy for the construction of **1** and **2** (b).

Results and Discussion

Synthesis and Characterization

It is well known that the reactions of silver(I) ions with polycarboxylates in aqueous solution often result in the formation of insoluble silver salts, presumably due to the rapid coordination of the carboxylate ions to the silver ions to form polymeric structures. Mak and co-workers have generated polymeric structures in silver(I) carboxylate like complexes by using various zwitterionic betaine-type ligands,[11] and Smith and co-workers[12] have obtained a series of Ag polycarboxylate complexes by using ammonia to enhance the solubility of the silver carboxylates. Similarly, Michaelides and co-workers[13] have reported a novel succinatodisilver(I) complex synthesized by gel permeation. Hence, it appears that the correct choice of reaction conditions may result in the formation of crystalline products that are suitable for X-ray structural analysis. 2,1,3-Benzoselenadiazole (bsd) can coordinate to metal ions through two N atoms in a monodentate or μ_2-bridging mode (Scheme 2). Moreover, the uncoordinated N atom can form a weak Se···N interaction which could help in the construction of the framework (Scheme 2a).[10] In light of all this, we treated freshly synthesized $[Ag(NH_3)_2](OH)$ and H_3btc/H_3ctc ligand with bsd (4:1:4 molar ratio), which resulted in the formation of complexes **1** and **2**, respectively, which possess hexagonal Ag^I(btc/ctc) coordination networks. The auxiliary bsd ligand plays a vital role in the formation of these networks. It should be noted that complicated silver(I) complexes containing btc^{3-} or $Hbtc^{2-}$ ligands have been documented previously.[14]

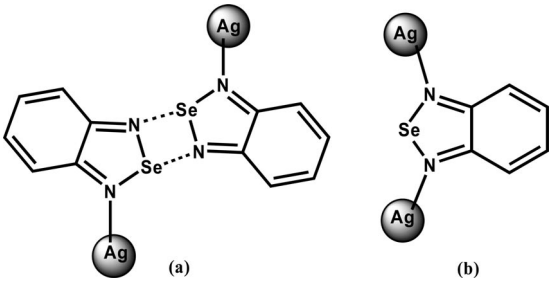

Scheme 2. Coordination modes of the bsd ligand: monodentate with an Se···N nonbonding interaction (a) and a μ_2-bridging mode (b).

Crystal Structure

The X-ray structural analysis reveals that **1** crystallizes in the monoclinic $P2_1/c$ space group with an asymmetric unit that contains three Ag^I atoms, one btc^{3-} ligand, six monodentate bsd ligands (one of which shows twofold disorder) and half a lattice water molecule (Figure 1). Selected bond lengths and angles are listed in Table 1. Ag1 is coordinated in a strongly distorted tetrahedral environment to two O atoms from two btc^{3-} anions and two N atoms from two bsd ligands [Ag1–O 2.240(6) and 2.244(6) Å; Ag1–N 2.30(1) and 2.384(6) Å; N/O–Ag1–O/N 89.6(2)–146.2(2)°]. It also has an Ag···Ag contact[15] [2.872(1) Å]. Ag2 is also coordinated in a strongly distorted tetrahedral coordination geometry and is surrounded by two O atoms from two btc^{3-} anions and two N atoms from two bsd ligands [Ag2–O 2.532(5) and 2.566(5) Å; Ag2–N 2.203(6) and 2.211(6) Å; N/O–Ag2–O/N 77.2(2)–164.6(2)°] and also forms one weak Ag–O interaction (Ag2–O6 2.729 Å), while Ag3 is coordi-

nated to one O atom from one btc^{3-} ligand and two N atoms from two bsd ligands in a Y-shaped coordination geometry [Ag3–O 2.372(5) Å; Ag3–N 2.204(6) and 2.205(6) Å; N/O–Ag3–N 94.4(2)–161.6(2)°], as well as forming one weak Ag–O interaction (Ag3–O6 2.657 Å). Each btc^{3-} ligand acts in a μ_6-bridging mode to connect six Ag^I atoms, and each Ag_2 dimer is coordinated by two btc^{3-} ligands via *syn,syn-O,O′* bridges and single O-bridges to form 2D honeycomb layers (Figure 2a) containing highly deformed hexagonal rings (Figure 2b). Each of these rings contains six Ag_2 dimers and six btc^{3-} ligands. There are twelve bsd ligands coordinated to each hexagonal ring, ten of which orient themselves perpendicular to the hexagonal net. The other two are located within the hexagonal net and

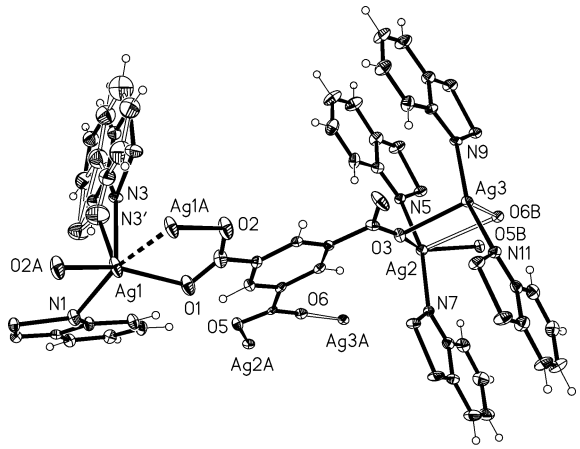

Figure 1. Perspective views of the coordination geometries of the Ag^I ions and the bridging mode of the btc^{3-} ligand in **1**.

Table 1. Selected bond lengths [Å] and angles [°] for **1** and **2**.[a]

Complex **1**			
Ag(1)–O(2a)	2.240(6)	Ag(2)–O(5b)	2.532(5)
Ag(1)–O(1)	2.244(6)	Ag(2)–O(3)	2.566(5)
Ag(1)–N(3)	2.295(11)	Ag(3)–N(11)	2.204(6)
Ag(1)–N(1)	2.384(6)	Ag(3)–N(9)	2.205(6)
Ag(2)–N(5)	2.203(6)	Ag(3)–O(3)	2.372(5)
Ag(2)–N(7)	2.211(6)	Ag(1)···Ag(1a)	2.8722(13)
O(2a)–Ag(1)–O(1)	146.2(2)	N(7)–Ag(2)–O(5b)	104.12(19)
O(2a)–Ag(1)–N(3)	106.4(3)	N(5)–Ag(2)–O(3)	104.54(18)
O(1)–Ag(1)–N(3)	98.2(4)	N(7)–Ag(2)–O(3)	77.24(19)
O(2a)–Ag(1)–N(1)	89.6(2)	O(5b)–Ag(2)–O(3)	143.11(16)
O(1)–Ag(1)–N(1)	103.4(2)	N(11)–Ag(3)–N(9)	161.6(2)
N(3)–Ag(1)–N(1)	110.3(3)	N(11)–Ag(3)–O(3)	94.4(2)
N(5)–Ag(2)–N(7)	164.6(2)	N(9)–Ag(3)–O(3)	101.9(2)
N(5)–Ag(2)–O(5b)	83.76(19)		
Complex **2**			
Ag(1)–O(2a)	2.225(4)	Ag(1)–O(1)	2.427(3)
Ag(1)–N(1)	2.291(5)	Ag(1)···Ag(1a)	2.9461(9)
Ag(1)–N(2b)	2.346(4)		
O(2a)–Ag(1)–N(1)	120.13(18)	N(1)–Ag(1)–O(1)	81.77(14)
O(2a)–Ag(1)–N(2b)	112.16(17)	N(2b)–Ag(1)–O(1)	72.27(16)
O(2a)–Ag(1)–O(1)	149.98(16)		

[a] Symmetry codes: a: $-x - 1, -y + 2, -z + 1$; b: $-x, y + 1/2, -z + 3/2$ for **1**; a: $-x + 1, -y + 2, -z + 1$; b: $y - 1/3, -x + y + 1/3, -z + 4/3$ for **2**.

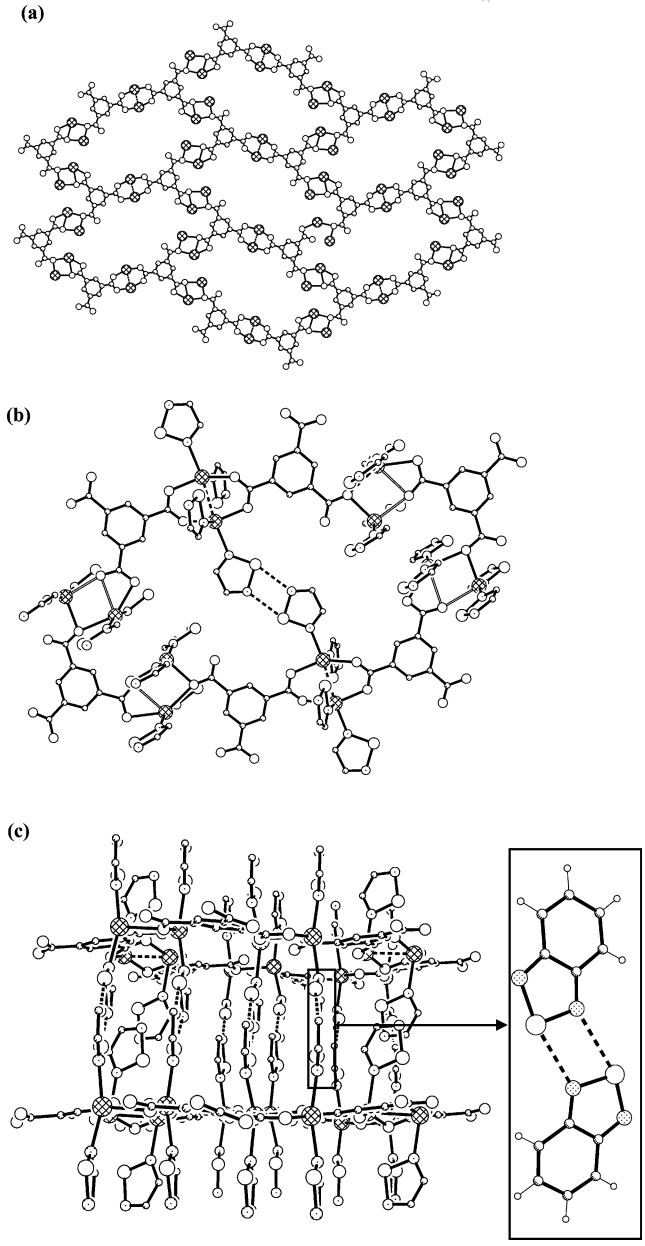

Figure 2. View of the highly deformed $Ag_6(btc)_6$ hexagonal circle (a), the 2D honeycomb net (bsd ligand have been omitted for clarity) (b) and the 3D supramolecular architecture formed by interlayer $(bsd)_2$ bridges containing self-complementary Se···N synthons (c) in **1**. Some carbon atoms of the bsd ligands in (b) and (c) have been omitted for clarity. Atom types: Ag: cross-hatched circle; Se: large open circle; O: small circle; N: circle with regular dot pattern; C: shaded circle with highlight.

are stabilized by a self-complementary Se···N interaction[10] [Se···N 2.855(1) Å]. The 2D hexagonal nets are further extended into a 3D supramolecular architecture (Figure 2c) via self-complementary Se···N interactions [Se···N 2.849(1) and 2.950(1) Å] between the interlayer dangling bsd groups. To the best of our knowledge, only one 3D molecular framework has been generated by self-complementary Se···N interactions between a pair of bsd molecules.[10]

The X-ray structural analysis of **2** reveals that it crystallizes in the rhombohedral space group $R\bar{3}$. The asymmetric unit consists of a unique Ag^{I} atom, which lies in a general position, one-third of a ctc^{3-} ligand, which lies across the a $\bar{3}$-axis, one twofold disordered bsd ligand due to rotation about the N–N axis, a disordered bsd molecule with an occupancy of 0.5 and water guests (Figure 3a). Ag1 is coordinated in a strongly distorted tetrahedral environment to two O atoms from two ctc^{3-} ligands and two N atoms from two bsd ligands [Ag1–O 2.226(6) and 2.426(5) Å; Ag1–N 2.293(8) and 2.33(2)/2.38(2) Å; N/O–Ag1–O/N 72.1(5)–149.9(2)°]. It also forms an Ag···Ag contact [2.9461(9) Å]. As in **1**, each ctc^{3-} ligand acts as a μ_6-bridge to connect three Ag_2 dimers into ideal 2D honeycomb nets, with each hexagonal unit consisting of six trigonal ctc^{3-} ligands and six Ag_2 dimers (Figure 3b, Scheme 1b). In our previous investigation on the assembly of coordination polymers with metal clusters as building blocks, $Ag_2(MeCO_2)_2$ was used as a secondary building unit for the construction of 3D MOFs.[15] The 2D hexagonal nets of **2** are further connected by μ_2-bridging bsd ligands into a 3D MOF (Figure 4a) which is quite different from that in **1**. Interestingly, this 3D MOF can also be deconstructed into two types of nanoscale cage units, namely $Ag_{24}(ctc)_2(bsd)_{12}$ and $Ag_{12}(ctc)_2(bsd)_6$ (Figure 4b and c and Figure S1 in the Supporting Information). Each $Ag_{24}(ctc)_2(bsd)_{12}$ cage has the dimensions $13.38 \times 14.23 \times 16.48$ Å^3 and contains a pair of $Ag_6(ctc)$ motifs and six $Ag_2(\mu\text{-bsd})_2$ motifs, and each $Ag_{12}(ctc)_2(bsd)_6$ cage contains a pair of $Ag_6(ctc)$ motifs and six μ-bsd motifs. The void volume (V_{void}) of **2** without guests is 21.5% per unit volume, as calculated by PLATON.[16] The twofold disordered bsd guest molecules are located in the windows of the larger cages and interact with the host through Se···O nonbonding interactions (Se2···O2^i 3.054 Å; symmetry code: $i = 1/3 - x$, $5/3 - y$, $2/3 - z$)[17a,17b] as well as an edge-to-face interaction[17c] involving bsd(host)···bsd(guest) motifs (Figure 4d).

The network topology can be simplified by considering the 6-connected dimeric Ag_2 units and the 3-connected ctc^{3-} ligands as octahedral and trigonal nodes, respectively; the bidentate bsd ligands can be represented simply as links between the Ag_2 nodes. The resulting net is shown in Figure 4e, which is a new (3,6)-connected net[1d] with octahedral and trigonal nodes in a 3:2 ratio. The long topological (O'Keeffe) vertex symbol is $4.4.4.4.4.4.6_2.6_2.6_2.6_2.6_4.6_4.8_4.8_4.*$[18] for the Ag_2 node and 4.4.4 for the ctc^{3-} node, which gives the short vertex symbol $(4^3)_2(4^6.6^6.8^3)_3$.

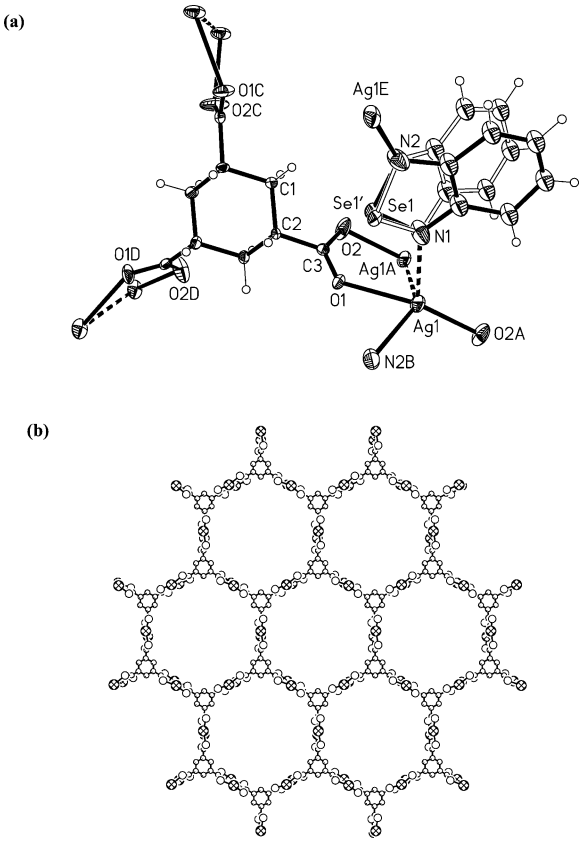

Figure 3. Perspective views of the coordination geometry of the Ag^{I} ion and the bridging mode of the ctc^{3-} ligand (a) and the 2D $Ag_3(ctc)$ honeycomb net along the *c*-axis (b) in **2**.

Thermogravimetric Analysis

We carried out thermal gravimetric (TG) analyses to examine the thermal stabilities of the networks and measured the XPRD patterns to confirm the purity of the two complexes (Figure 5). Samples of the complexes were heated under nitrogen to 500 °C. The TGA curve of **1** (Figure 6a) shows that this complex is stable up to 110 °C, with the small weight loss of 0.6% at about 105 °C corresponding to the loss of the half lattice water molecule (calculated: 0.6%). The second weight loss of 45.2% between 110 and 172 °C is in accordance with loss of the four bsd ligands of the unit cell (calculated: 44.7%) that lie between the adjacent hexagonal layers. Gradual loss of the other two bsd ligands and btc^{3-} ligands occurs above 172 °C, and the complex decomposes completely to Ag_2O (found: 21.4%; calculated: 21.2%) up to 385 °C. Complex **2** is less stable than **1** due to its porous network and many guest molecules. The TGA curve of **2** (Figure 6b) shows loss of two of the lattice water molecules (found: 2.4%; calculated: 2.5%) at about 55 °C, with the others (1.9%) being lost up to 130 °C (calculated: 1.8%). The second weight loss of 39.4% between 130 and 180 °C corresponds to the loss of guest bsd molecules and one and a half of the coordinated ligands (calculated: 38.5%). The remaining half of the coordinated bsd ligand (5.9%) is lost between 180 and 240 °C (calculated: 6.4%). The final weight loss of 12.7% up to 265 °C occurs due to loss of the last bsd ligand, and the complex finally decomposesd to Ag_2O residue (found: 25.1%; calculated: 24.4%) up to 300 °C. Four endothermic peaks in the DTA curve also indicate the loss of various groups.

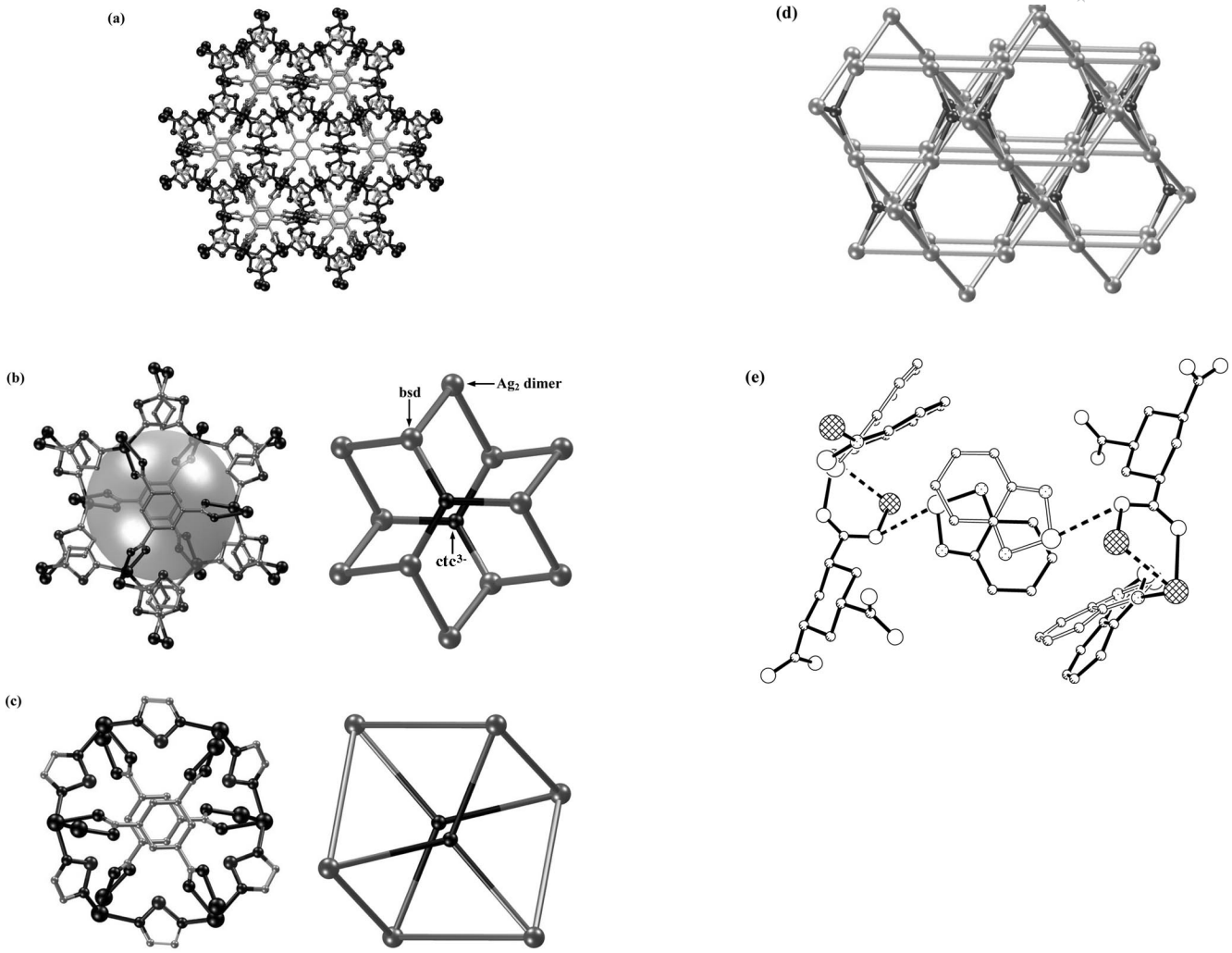

Figure 4. Top-views of the 3D cage-based network (a), the nanoscale $Ag_{24}(ctc)_2(bsd)_{12}$ cage (b) and the $Ag_{12}(ctc)_2(bsd)_6$ cage (c), the (3,6)-connected topological net (d), and the bsd(host)···bsd(guest) interaction (e) in **2**. Some carbon atoms of of the bsd ligands in (b) and (c) have been omitted for clarity. Atom types: Ag: cross-hatched circle; Se: large open circle; O: small circle; N: circle with regular dot pattern; C: shaded circle with highlight.

Conclusions

The presence of bsd as an auxiliary ligand leads to the formation of two novel MOFs containing 2D hexagonal net motifs, namely $[Ag_3(btc)(bsd)_6]\cdot 0.5H_2O$ (**1**) and $[Ag_3(ctc)(bsd)_3]\cdot 1.5bsd\cdot 3.5H_2O$ (**2**), from the reaction of freshly synthesized $[Ag(NH_3)_2](OH)$ with H_3btc or H_3ctc at room temperature. Complex **1** is a 3D supramolecular framework that is formed by interlayer Se···N interactions between the dangling monodentate bsd groups of 2D neutral deformed honeycomb-like $Ag_3(btc)$ layers, whereas **2** is a 3D metal–organic framework containing nanoscale cages between ideal $Ag_3(ctc)$ honeycomb layers and μ_2-bridging bsd ligands. Complex **2** is a new (3,6)-connected topological net.

Experimental Section

General Remarks: All reagents and solvents employed were commercially available and were used as received without further purification. The C, H, and N microanalyses were carried out with an Elementar Vario-EL CHNS elemental analyzer. The IR spectra were recorded from KBr pellets in the range 4000–400 cm^{-1} with a Bio-Rad FTS-7 spectrometer. X-ray powder diffraction (XPRD) intensities for **1** and **2** were measured at 293 K with a Rigaku D/max-IIIA diffractometer (Cu-K_α, λ = 1.54056 Å). Crushed single-crystalline powder samples were prepared and scanned from 5–65° with a step of 0.1° per second. Thermal gravimetry (TG) was carried out with a NETZSCH TG209F3 thermal gravimetric analyzer, by heating the samples from 30–500 °C at a rate of 10 °C min^{-1}.

Synthesis of 1 and 2: Excess aqueous NH_3 solution was slowly added dropwise to a suspension of Ag_2O (0.116 g, 0.5 mmol) in $MeCN/H_2O$ (15 mL, 2:1 v/v) and the mixture stirred for 15 min. H_3btc (0.053 g, 0.25 mmol) or H_3ctc (0.054 g, 0.25 mmol) and 2,1,3-benzoselenadiazole (bsd) ligand (0.183 g, 1.0 mmol) were then slowly added, and the mixture was stirred for 30 min. The resultant colorless solution was allowed to stand in the dark at room temperature for a week to give yellow block crystals of **1** (yield: 0.340 g, ca. 83% based on H_3btc) or **2** (yield: 0.284 g, ca. 80% based on H_3ctc). **1:** $C_{45}H_{28}Ag_3N_{12}O_{6.5}Se_6$ (1638.2): calcd. C

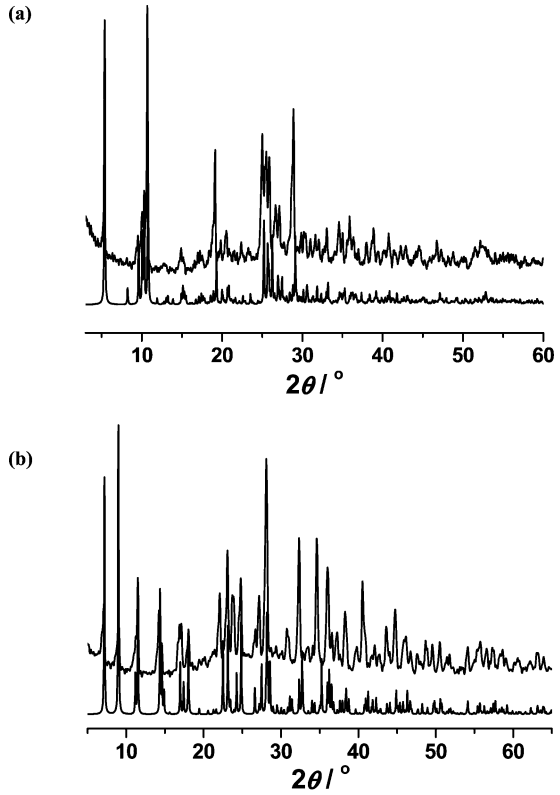

Figure 5. Observed (gray) and calculated (black) X-ray powder diffraction patterns for **1** (a) and **2** (b).

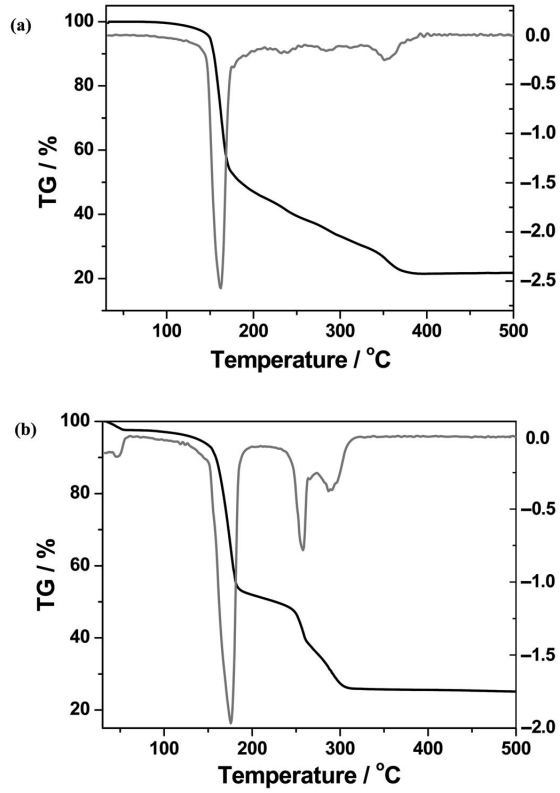

Figure 6. TGA (black) and DTA (gray) curves for **1** (a) and **2** (b).

Table 2. Crystal and structure refinement data for complexes **1** and **2**.[a]

Compound	**1**	**2**
Empirical formula	$C_{45}H_{28}Ag_3N_{12}O_{6.5}Se_6$	$C_{36}H_{34}Ag_3N_9O_{9.5}Se_{4.5}$
Formula mass	1638.16	1423.65
Temperature [K]	123(2)	173(2)
Wavelength [Å]	0.71073	0.71073
Crystal system	monoclinic	rhombohedral
Space group	$P2_1/c$	$R\bar{3}$
a [Å]	10.7459(8)	19.662(1)
b [Å]	13.866(1)	19.662(1)
c [Å]	32.827(2)	17.839(2)
α [°]	90	90
β [°]	92.846(1)	90
γ [°]	90	120
V [Å^3]	4885.2(6)	5972.4(7)
Z	4	6
Calculated density [g cm^{-3}]	2.227	2.375
Absorption coefficient [mm^{-1}]	5.725	5.646
F(000)	3116	4098
Crystal size [mm]	0.18 × 0.11 × 0.05	0.16 × 0.12 × 0.08
θ range for data collection [°]	1.90–26.00	1.65–27.75
Limiting indices	$-5 \leq h \leq 13$	$-21 \leq h \leq 25$
	$-17 \leq k \leq 16$	$-25 \leq k \leq 25$
	$-40 \leq l \leq 38$	$-21 \leq l \leq 23$
Reflections collected/unique	23987/9569	10899/2937
Completeness	99.5% (θ_{max} = 26.00°)	93.5% (θ_{max} = 27.75°)
Absorption correction	multi-scan (*SADABS*, Bruker, **2002**)	multi-scan (*SADABS*, Bruker, **2002**)
Max. and min transmission	0.4222/0.7628	0.6609/0.4653
Refinement method	full-matrix least squares on F^2	full-matrix least squares on F^2
Data/restrains/parameters	9569/136/703	2937/86/196
Goodness-of-fit on F^2	0.935	1.095
R indexes [$I > 2\sigma(I)$]	R_1 = 0.0522, wR_2 = 0.1205	R_1 = 0.0687, wR_2 = 0.2070
R indices (all data)	R_1 = 0.0755, wR_2 = 0.1278	R_1 = 0.0844, wR_2 = 0.2184
Largest diff. peak/hole [e Å^{-3}]	1.636/–2.202	2.479/–2.091

[a] $R_1 = \Sigma||F_o| - |F_c||/\Sigma|F_o|$, $wR_2 = [\Sigma w(F_o^2 - F_c^2)^2/\Sigma w(F_o^2)^2]^{1/2}$.

32.99, H 1.72, N 10.26; found C 33.34, H 1.63, N 10.70. IR (KBr): $\tilde{\nu}$ = 3403 (w), 3081 (w), 3054 (w, 3010 (w), 1602 (s), 1542 (vs), 1509 (m), 1481 (m), 1425 (w), 1135(w), 1090 (w), 981 (w), 950 (w), 848 (w), 807 (w), 744 (vs), 711 (vs), 596 (w), 556 (w), 518 (w) cm^{-1}. **2:** $C_{36}H_{34}Ag_3N_9O_{9.5}Se_{4.5}$ (1423.7) : calcd. C 30.37, H 2.41, N 8.85; found C 30.07, H 2.29, N 8.71. IR (KBr): $\tilde{\nu}$ = 3379 (s), 2945 (w), 1655 (w), 1560 (vs), 1511 (m), 1479 (w), 1393 (s), 1351m), 1292 (w, 1213w), 1132 (w, 1021 (w), 973 (w), 916 (w), 772 (w), 745 (vs), 597 (w), 578 (w) cm^{-1}.

X-ray Crystallographic Study: Diffraction intensities for **1** and **2** were collected with a Bruker Apex CCD area-detector diffractometer (Mo-K_α, λ = 0.71073 Å). Absorption corrections were applied by using the multiscan program SADABS.[19] The structures were solved by direct methods and refined with a full-matrix least-squares technique with the SHELXTL program package.[20] Anisotropic thermal parameters were applied to all non-hydrogen atoms. Hydrogen atoms were placed at calculated positions and were included in the refinement in the riding model approximation, with U set to 1.2- or 1.5-times those of the parent atoms. For **2**, the bsd ligand was treated as being twofold disordered around the N–N axis of bsd, with the disordered atoms Se1, C4, C5, C6, C7, C8, C9 and Se1′, C4′, C5′, C6′, C7′, C8′, C9′ each having an occupancy of 50%. The crystallographic data for **1** and **2** are listed in Table 2. **1:** $C_{45}H_{28}Ag_3N_{12}O_{6.5}Se_6$, M = 1638.16, monoclinic, space group $P2_1/c$ (no. 14), a = 10.746(1), b = 13.866(1), c = 32.827(2) Å, β = 92.846(1)°, V = 4885.2(6) $Å^3$, Z = 4, T = 123(2) K, $F(000)$ = 3116, D_c = 2.227 $g\,cm^{-3}$, μ(Mo-K_α) = 5.725 mm^{-1}; R_1 = 0.0522, wR_2 = 0.1205 and GOF = 0.935 for 703 parameters, 6598 reflections with $|F_o| \geq 4\sigma(F_o)$. **2:** $C_{36}H_{34}Ag_3N_9O_{9.5}Se_{4.5}$, M = 1423.65, rhombohedral, space group $R\bar{3}$ (no. 148), a = 19.662(1), c = 17.839(2) Å, V = 5972.4(7) $Å^3$, Z = 6, T = 173(2) K, $F(000)$ = 4098, D_c = 2.375 $g\,cm^{-3}$, μ(Mo-K_α) = 5.646 mm^{-1}; R_1 = 0.0687, wR_2 = 0.2070 and GOF = 1.095 for 196 parameters, 2228 reflections with $|F_o| \geq 4\sigma(F_o)$. CCDC-628822 (**1**) and -628823 (**2**) contain the supplementary crystallographic data for this paper. These data can be obtained free of charge from The Cambridge Crystallographic Data Center via www.ccdc.cam.ac.uk/data_request/cif.

Supporting Information (see footnote on the first page of this article): Side-view of the $Ag_{24}(ctc)_2(bsd)_{12}$ cage and topological net viewed along the c-axis in **2**.

Acknowledgments

This work was supported by the National Natural Science Foundation of China (grant nos. 20525102 and 20471069), the Foundation for the Author of National Excellent Doctoral Dissertation of China (200122), and the Scientific and Technological Project of Guangdong Province (04205405).

[1] a) B. Moulton, M. J. Zaworotko, *Chem. Rev.* **2001**, *101*, 1629–1645; b) S. R. Batten, *CrystEngComm* **2001**, *3*, 1–8; c) S. Kitagawa, R. Kitaura, S.-i. Noro, *Angew. Chem. Int. Ed.* **2004**, *43*, 2334–2375; d) V. A. Blatov, L. Carlucci, G. Ciani, D. M. Proserpio, *CrystEngComm* **2004**, *6*, 378–395; e) M. J. Zaworotko, *Chem. Commun.* **2001**, 1–9; f) R. J. Hill, D. L. Long, N. R. Champness, P. Hubberstey, M. Schröder, *Acc. Chem. Res.* **2005**, *38*, 337–350.

[2] a) T. M. Reineke, M. Eddaoudi, D. Moler, M. O'Keefe, O. M. Yaghi, *J. Am. Chem. Soc.* **2000**, *122*, 4843–4844; b) D.-L. Long, A. J. Blake, N. R. Champness, C. Wilson, M. Schröder, *J. Am. Chem. Soc.* **2001**, *123*, 3401–3402; c) K. G. Nath, O. Ivasenko, J. A. Miwa, H. Dang, J. D. Wuest, A. Nanci, D. F. Perepichka, F. Rosei, *J. Am. Chem. Soc.* **2006**, *128*, 4212–4213.

[3] a) O. M. Yaghi, H. Li, T. L. Groy, *J. Am. Chem. Soc.* **1996**, *118*, 9096–9097; b) S. S. Y. Chui, S. M. F. Lo, J. P. H. Charmant, A. G. Orpen, I. D. Williams, *Science* **1999**, *283*, 1148–1150.

[4] a) C. V. K. Sharma, M. J. Zaworotko, *Chem. Commun.* **1996**, 2655–2656; b) T. R. Shattock, P. Vishweshwar, Z. Wang, M. J. Zaworotko, *Cryst. Growth Des.* **2005**, *5*, 2046–2049; c) P. Vishweshwar, D. A. Beauchamp, M. J. Zaworotko, *Cryst. Growth Des.* **2006**, *6*, 2429–2431; d) I. Goldberg, J. Bernstein, *Chem. Commun.* **2007**, 132–134.

[5] a) B. R. Bhogala, P. Vishweshwar, A. Nangia, *Cryst. Growth Des.* **2002**, *2*, 325–328; b) B. R. Bhogala, A. Nangia, *Cryst. Growth Des.* **2003**, *3*, 547–554; c) B. R. Bhogala, A. Nangia, *Cryst. Growth Des.* **2006**, *6*, 32–35.

[6] a) I. Ino, L. P. Wu, M. Munakata, M. Maekawa, Y. Suenaga, T. Kuroda-Sowa, Y. Kitamori, *Inorg. Chem.* **2000**, *39*, 2146–2152; b) K. A. Hirsch, S. R. Wilson, J. S. Moore, *Inorg. Chem.* **1997**, *36*, 2960–2967; c) H. Imai, H. Nakamura, T. Fukuyo, *Cryst. Growth Des.* **2005**, *5*, 1073–1077.

[7] a) P. L. Caradoc-Davies, L. R. Hanton, *Chem. Commun.* **2001**, 1098–1099; b) Y.-B. Xie, C. Zhang, J.-R. Li, X.-H. Bu, *Dalton Trans.* **2004**, 562–569; c) Y.-B. Xie, R.-H. Zhang, X.-H. Bu, *Cryst. Growth Des.* **2003**, *3*, 829–835.

[8] a) M. Maekawa, H. Konaka, Y. Suenaga, T. Kuroda-Sowa, M. Munakata, *J. Chem. Soc. Dalton Trans.* **2000**, 4160–4166; b) M.-L. Tong, S.-L. Zheng, X.-M. Chen, *Chem. Eur. J.* **2000**, *6*, 3729–3738; c) R. Alberto, D. Angst, U. Abram, K. Ortner, T. A. Kaden, A. P. Schubiger, *Chem. Commun.* **1999**, 1513–1514.

[9] a) K. S. Singh, J. R. Long, P. Stavropoulos, *J. Am. Chem. Soc.* **1997**, *119*, 2942–2943; b) L. Pan, E. B. Woodlock, X. T. Wang, K. C. Lam, A. L. Rheingold, *Chem. Commun.* **2001**, 1762–1763; c) O. Kristiansson, *Inorg. Chem.* **2001**, *40*, 5058–5066; d) M. A. Omary, T. R. Webb, Z. Assefa, G. E. Shankle, H. H. Patterson, *Inorg. Chem.* **1998**, *37*, 1380–1387; e) M.-L. Tong, X.-M. Chen, B.-H. Ye, *Inorg. Chem.* **1998**, *37*, 5278–5281; f) A. Erxleben, *Inorg. Chem.* **2001**, *40*, 2928–2931.

[10] A.-J. Zhou, S.-L. Zheng, Y. Fang, M.-L. Tong, *Inorg. Chem.* **2005**, *44*, 4457–4459.

[11] a) X. L. Zhao, Q. M. Wang, T. C. W. Mak, *Chem. Eur. J.* **2005**, *11*, 2094–2102; b) X. Zhang, G. C. Guo, F. K. Zheng, G. W. Zhou, J. G. Mao, Z. C. Dong, J. S. Huang, T. C. W. Mak, *J. Chem. Soc. Dalton Trans.* **2002**, 1344–1349; c) D. D. Wu, T. C. W. Mak, *J. Chem. Soc. Dalton Trans.* **1995**, 2671–2678; d) X. M. Chen, T. C. W. Mak, *J. Chem. Soc. Dalton Trans.* **1991**, 3253–3258; e) X. M. Chen, T. C. W. Mak, *J. Chem. Soc. Dalton Trans.* **1991**, 1219–1222.

[12] G. Smith, A. N. Reddy, K. A. Byriel, C. H. L. Kennard, *J. Chem. Soc. Dalton Trans.* **1995**, 3565–3570.

[13] A. Michaelides, V. Kiritsis, S. Skoulika, A. Aubry, *Angew. Chem. Int. Ed. Engl.* **1993**, *32*, 1495–1499.

[14] a) D. Sun, R. Cao, J. Weng, M. Hong, Y. Liang, *J. Chem. Soc. Dalton Trans.* **2002**, 291–292; b) D. Sun, R. Cao, W. Bi, J. Weng, M. Hong, Y. Liang, *Inorg. Chim. Acta* **2004**, *357*, 991–1001; c) B. Ding, L. Yi, Y. Liu, P. Cheng, Y.-B. Dong, J.-P. Ma, *Inorg. Chem. Commun.* **2005**, *8*, 38–40.

[15] J. Wang, S. Hu, M.-L. Tong, *Eur. J. Inorg. Chem.* **2006**, 2069–2077.

[16] A. L. Spek, *PLATON, A Multipurpose Crystallographic Tool*, Utrecht University, Utrecht, The Netherlands, **2001**.

[17] a) M. Iwaoka, H. Komatsu, T. Katsuda, S. Tomoda, *J. Am. Chem. Soc.* **2004**, *126*, 5309–5317; b) N. E. Chakov, W. Wernsdorfer, K. A. Abboud, G. Christou, *Inorg. Chem.* **2004**, *43*, 5919–5930; c) V. Russell, M. Scudder, I. Dance, *J. Chem. Soc. Dalton Trans.* **2001**, 789–799.

[18] D. Braga and J. Bernstein, *Networks, Topologies and Entanglements in Making Crystals by Design – Methods, Techniques, Ap-*

plications (Eds.: D. Braga, F. Grepioni), Wiley-VCH, Weinheim, **2006**, chapter 1.3, pp. 58–85.
[19] G. M. Sheldrick, *SADABS 2.05 – Program for Area Detector Absorption Correction*, University of Göttingen, Germany, **2002**.
[20] *SHELXTL 6.10*, Bruker Analytical Instrumentation, Madison, Wisconsin, USA, **2000**.

Received: September 6, 2007
Published Online: January 3, 2008

